STRESS INTENSITY AT A CRACK

BETWEEN BONDED DISSIMILAR MATERIALS[1]

Morris Stern and Chen-Chin Hong
The University of Texas at Austin

INTRODUCTION

The nature of the stress field in front of a crack lying in the surface between bonded dissimilar materials was first investigated by Williams (ref. 1). He observed that not only do the stresses grow at a rate inversely proportional to the square root of distance from the crack tip, they also exhibit an oscillatory singularity with wave length inversely proportional to the absolute value of the logrithm of distance from the crack tip. The problem of calculating stress intensity factors for various special loadings and geometries has been treated by other authors, among them Erdogan (ref. 2 and 3), England (ref. 4), Rice and Sih (ref. 5), and Erdogan and Gupta (ref. 6). In all cases for which results are given the region is unbounded and the loads are uniform.

For more general boundary value problems involving imperfect bonding of dissimilar materials numerical methods must be resorted to, and both the growth and oscillatory nature of the singularity can be expected to cause numerical difficulties. In addition, because the elastic moduli of the materials are generally different, discontinuities in components of stress and strain develop naturally on the bond. Recently we extended the contour integral method to problems of this type. It turns out that the nature of the loading and restraints, even on remote edges, can have a significant effect on the stress intensity. In this paper we treat some example problems to illustrate this.

The basic boundary value problem is illustrated in Fig. 1. Two dissimilar materials are joined along a straight edge with one or more cracks present. The composite is loaded or restrained on the remote boundary, and the crack faces are free of load. Local cartesian and polar coordinates are introduced with origin at a crack tip and the negative x-axis ($\theta = \pm \pi$) along the crack edges. The subscript 1 is arbitrarily assigned to material below the axis ($-\pi < \theta < 0$), and the subscript 2 is used for the other material ($0 < \theta < \pi$). Also introduced is the so-called bimaterial constant

$$\gamma = \frac{\mu_1 + \mu_2 \kappa_1}{\mu_2 + \mu_1 \kappa_2} \tag{1}$$

where μ_1, μ_2 are the respective shear moduli and $\kappa = 3-4\nu$ for plane strain, or $\kappa = (3-4\nu)(1+\nu)$ for plane stress, ν being Poisson's Ratic

Notation for complex displacement and stress fields in terms of components referred to the local polar coordinate system are introduced as follows:

$$u = u_r + iu_\theta$$

$$\sigma_r = \sigma_{rr} + i\tau_{r\theta} \tag{2}$$

$$\sigma_\theta = \sigma_{\theta\theta} - i\tau_{r\theta}$$

Then the displacement and stress fields in the neighborhood of the crack tip in each material are of the form[2]

$$u_1 = \frac{\bar{K}}{2\mu_1(1+\gamma)\lambda} r^\lambda [\kappa_1 e^{i(\lambda-1)\theta} - \gamma e^{i(-\lambda-1)\theta}]$$

$$+ \frac{K}{2\mu_1(1+\gamma)} r^{\bar{\lambda}} [e^{i(-\bar{\lambda}-1)\theta} - e^{i(-\bar{\lambda}+1)\theta}] + \text{remainder}$$

$$u_2 = \frac{\bar{K}}{2\mu_2(1+\gamma)\lambda} r^\lambda [\kappa_2 \gamma e^{i(\lambda-1)\theta} + e^{i(-\lambda-1)\theta}]$$

$$+ \frac{K}{2\mu_2(1+\gamma)} r^{\bar{\lambda}} [e^{i(-\bar{\lambda}+1)\theta} - e^{i(-\lambda+1)\theta}] + \text{remainder}$$

$$\sigma_{1r} = \frac{\bar{K}}{(1+\gamma)} r^{\lambda-1} [e^{i(\lambda-1)\theta} - \gamma e^{i(-\lambda-1)\theta}]$$

$$+ \frac{K}{(1+\gamma)} r^{\bar{\lambda}-1} [\bar{\lambda} e^{i(\bar{\lambda}-1)\theta} - (\bar{\lambda}-2) e^{i(-\bar{\lambda}+1)\theta}] + \text{remainder}$$

$$\sigma_{2r} = \frac{\bar{K}}{(1+\gamma)} r^{\lambda-1} [\gamma e^{i(\lambda-1)\theta} - e^{i(-\lambda-1)\theta}]$$

$$\tag{3}$$

$$+ \frac{K\gamma}{(1+\gamma)} r^{\bar{\lambda}-1} [\bar{\lambda} e^{i(-\bar{\lambda}-1)\theta} - (\bar{\lambda}-2) e^{i(-\bar{\lambda}+1)\theta}] + \text{remainder}$$

$$\sigma_{1\theta} = \frac{\bar{K}}{(1+\gamma)} r^{\lambda-1} [e^{i(\lambda-1)\theta} + \gamma e^{i(-\lambda-1)\theta}]$$

$$+ \frac{K\bar{\lambda}}{(1+\gamma)} r^{\bar{\lambda}-1} [e^{i(-\bar{\lambda}+1)\theta} - e^{i(-\bar{\lambda}-1)\theta}] + \text{remainder}$$

$$\sigma_{2\theta} = \frac{\bar{K}}{(1+\gamma)} r^{\lambda-1} [\gamma e^{i(\lambda-1)\theta} + e^{i(-\lambda-1)\theta}]$$

$$+ \frac{K\gamma\bar{\lambda}}{(1+\gamma)} r^{\bar{\lambda}-1} [e^{i(-\bar{\lambda}+1)\theta} - e^{i(-\bar{\lambda}-1)\theta}] + \text{remainder}$$

---

[2] Except for notational differences these results were also obtained in references 3, 4 and 5.

where

$$\lambda = \frac{1}{2} + \frac{i}{2\pi} \ln \gamma = \frac{1}{2} + i\varepsilon \quad (\varepsilon = \frac{1}{2\pi} \ln \gamma) \tag{4}$$

and $K = K_o e^{i\beta}$ is a complex stress intensity factor with the following "physical" interpretation:

$$\lim_{r \to 0} \sigma_\theta \Big|_{\theta=0} = \lim_{x \to 0^+} (\sigma_{yy} - i\tau_{xy}) \Big|_{y=0}$$

$$= Kr^{\lambda-1} = K_o r^{-\frac{1}{2}} e^{i(\varepsilon \ln r + \beta)}$$

hence on the bond immediately in front of the crack tip we have

$$\sigma_{yy} = \frac{K_o}{\sqrt{r}} \cos(\varepsilon \ln r + \beta) + \text{remainder}$$

$$\tag{5}$$

$$\tau_{xy} = \frac{K_o}{\sqrt{r}} \sin(\varepsilon \ln r + \beta) + \text{remainder}$$

Thus K_o governs the amplitude growth rate of both the normal stress and shear stress while β determines a nonsignificant phase shift. The complex crack opening displacement is also governed by the stress intensity factor:

$$\Delta u = u_2 \Big|_{\theta=\pi} - u_1 \Big|_{\theta=-\pi} = \left\{ \frac{\mu_1 + \mu_2 \kappa_1}{\mu_1 \mu_2} \right\} \frac{\cosh \varepsilon\pi}{(1+\gamma)\lambda} \bar{K} r^\lambda$$

The amplitude of the complex crack opening displacement can be put in the form

$$|\Delta u| = \frac{(\mu_1 + \mu_2 \kappa_1)(\mu_2 + \mu_1 \kappa_2)}{\mu_1 \mu_2 (\mu_1 + \mu_2 + \mu_1 \kappa_2 + \mu_2 \kappa_1)} \frac{\cosh \varepsilon\pi}{\sqrt{\frac{1}{4} + \varepsilon^2}} K_o \sqrt{r} \tag{6}$$

A contour integral representation for the stress intensity factor is obtained from the reciprocal work identity by introducing a suitable artificial singular elastic state. Briefly, we observe that for arbitrary values of the complex constant C,

a singular elastic state corresponding to zero body force and with no traction on the lines $\theta = \pm \pi$ is defined in the bimaterial region by

$$2\mu_1 u_1^* = \bar{C}\lambda r^{-\lambda}[e^{i(\lambda+1)\theta} - e^{i(\lambda-1)\theta}]$$

$$+ Cr^{-\bar{\lambda}}[\kappa_1 e^{i(-\bar{\lambda}-1)\theta} - \gamma e^{i(\bar{\lambda}-1)\theta}]$$

$$2\mu_2 u_2^* = \bar{C}\lambda\gamma r^{-\lambda}[e^{i(\lambda+1)\theta} - e^{i(\lambda-1)\theta}]$$

$$+ Cr^{-\bar{\lambda}}[\kappa_2 \gamma e^{i(-\bar{\lambda}-1)\theta} - e^{i(\bar{\lambda}-1)\theta}]$$

$$\sigma_{r1}^* = \bar{C}\lambda r^{-\lambda-1}[\lambda e^{i(\lambda-1)\theta} - (\lambda+2)e^{i(\lambda+1)\theta}]$$

$$+ C\bar{\lambda}r^{-\bar{\lambda}-1}[\gamma e^{i(\bar{\lambda}-1)\theta} - e^{i(-\bar{\lambda}-1)\theta}]$$

$$\sigma_{r2}^* = \bar{C}\gamma\lambda r^{-\lambda-1}[\lambda e^{i(\lambda-1)\theta} - (\lambda+2)e^{i(\lambda+1)\theta}]$$

$$+ C\bar{\lambda}r^{-\bar{\lambda}-1}[e^{i(\bar{\lambda}-1)\theta} - \gamma e^{i(-\bar{\lambda}-1)\theta}]$$

$$\sigma_{\theta 1}^* = \bar{C}\lambda^2 r^{-\lambda-1}[e^{i(\lambda+1)\theta} - e^{i(\lambda-1)\theta}]$$

$$- C\bar{\lambda}r^{-\bar{\lambda}-1}[e^{i(-\bar{\lambda}-1)\theta} + \gamma e^{i(\bar{\lambda}-1)\theta}]$$

$$\sigma_{\theta 2}^* = \bar{C}\gamma\lambda^2 r^{-\lambda-1}[e^{i(\lambda+1)\theta} - e^{i(\lambda-1)\theta}]$$

$$- C\bar{\lambda}r^{-\bar{\lambda}-1}[\gamma e^{i(-\bar{\lambda}-1)\theta} + e^{i(\bar{\lambda}-1)\theta}]$$

(7)

This elastic state has the further property that on the contour C_ε (a circle of radius ε centered on the origin) we calculate a finite contribution from the reciprocal work as the contour shrinks to a point:

$$I_{tip} = \lim_{\epsilon \to 0} \int_{C_\epsilon} (\underset{\sim}{u}^* \cdot \underset{\sim}{t} - \underset{\sim}{u} \cdot \underset{\sim}{t}^*)\,ds$$

$$= \lim_{\epsilon \to 0} \int_{C_\epsilon} Re\,[\bar{u}^* \sigma_r - \bar{u}\sigma_r^*]\,ds \qquad (8)$$

$$= \frac{-\pi(\mu_1 + \mu_2 \kappa_1)}{\mu_1 \mu_2}\, Re\,\bar{C}K$$

Upon noting that the reciprocal work vanishes on the complete contour $C_o \cup C^+ \cup C_\epsilon \cup C^-$ indicated in Fig. 1 as a consequence of Betti's theorem, and on the crack edges $C^+ \cup C^-$ since the tractions in any case vanish there, we obtain the representation

$$\begin{Bmatrix} Re\ K \\ Im\ K \end{Bmatrix} = \int_{C_o} (\underset{\sim}{u} \cdot \underset{\sim}{t}^* - \underset{\sim}{u}^* \cdot \underset{\sim}{t})\,ds \qquad (9)$$

where for Re K we choose $C = -\dfrac{\mu_1 \mu_2}{\pi(\mu_1 + \mu_2 \kappa_1)}$ in Eq. (7) in calculating $\underset{\sim}{t}^*$ and $\underset{\sim}{u}^*$, whereas for Im K we take $C = -i\,\dfrac{\mu_1 \mu_2}{\pi(\mu_1 + \mu_2 \kappa_1)}$.

The values of $\underset{\sim}{u}$ and $\underset{\sim}{t}$ on the contour C_o are obtained numerically. For the results given in this paper we used code TEXGAP (ref. 7) which performs isotropic linearly elastic plane analyses using conventional quadratic displacement triangles and isoparametric quadrilaterals.

NUMERICAL RESULTS

The four cases treated involve a finite bimaterial strip loaded in tension and are sketched in Fig. 2. From symmetry considerations we need to consider only the shaded region, and in Fig. 3 we show a typical grid (symmetrically defined in each half region) for the finite element analyses. Half the contour used for evaluation of the stress intensity factors is shown in dashed line in Fig. 3. We note that the four distinct problems considered are obtained from the same grid and boundary conditions on the edges parallel to the crack, but with the following boundary conditions on the vertical edges:

704

i) Central crack - free edges: AB restrained, CD unrestrained
ii) Central crack - fixed edges: AB and CD restrained
iii) Single edge crack: AB and CD unrestrained
iv) Double edge crack: AB unrestrained, CD restrained.

Two sets of results are plotted in Fig. 4 and 5. The first shows the effect of different crack sizes in a given strip for each case; the second shows the effect of changing the relative dimensions of the strip for a fixed crack length to width ratio. In each case the results are normalized using the stress intensity factor for an infinite region loaded uniformly in tension normal to the crack and restrained from motion parallel to the crack on the remote boundary. This case is equivalent to an infinite bimaterial plate with vanishing stresses at infinity and a uniformly pressurized crack on the bond, for which analytical results are given in references (4) and (5):

$$K_\infty = \sqrt{1 + 4\varepsilon^2} \quad \sigma_o \sqrt{a/2} \tag{10}$$

It is interesting to note that for real materials the bimaterial constant γ is restricted to values between 1 and 3; consequently, the maximum variation in K_∞ that can be achieved by varying the properties of the two materials (this enters only through the parameter ε) is less than six percent, thus the isotropic case furnishes an excellent (lower bound) estimate for K_∞. The data plotted in Fig. 4 and 5 are based on material properties

$$\kappa_1 = 1.6, \quad \kappa_2 = 1.8, \quad \mu_2/\mu_1 = 17$$

which yields the value $\gamma = 1.5$.

REFERENCES

1. Williams, M.L.: The Stresses Around a Fault or Crack in Dissimilar Media. Bulletin of the Seismological Society of America, vol. 49, 1959, pp. 199-204.

2. Erdogan, F.: Stress Distribution in a Nonhomogeneous Elastic Plane With Cracks. Journal of Applied Mechanics, vol. 30, 1963, pp. 232-236.

3. Erdogan, F.: Stress Distribution in Bonded Dissimilar Materials With Cracks. Journal of Applied Mechanics, vol. 32, 1965, pp. 403-410.

4. England, A.H.: A Crack Between Dissimilar Media. Journal of Applied Mechanics, vol. 32, 1965, pp. 400-402.

5. Rice, J.R.; Sih, G.C.: Plane Problems of Cracks in Dissimilar Media. Journal of Applied Mechanics, vol. 32, 1965, pp. 418-423.

6. Erdogan, F.; Gupta, G.D.: Layered Composites with an Interface Flaw. International Journal of Solids and Structures, vol. 7, 1971, pp. 1089-1107.

7. Dunham, R.S.; Becker, E.B.: TEXGAP, The Texas Grain Analysis Program. TICOM Report 73-1, The University of Texas at Austin, August, 1973.
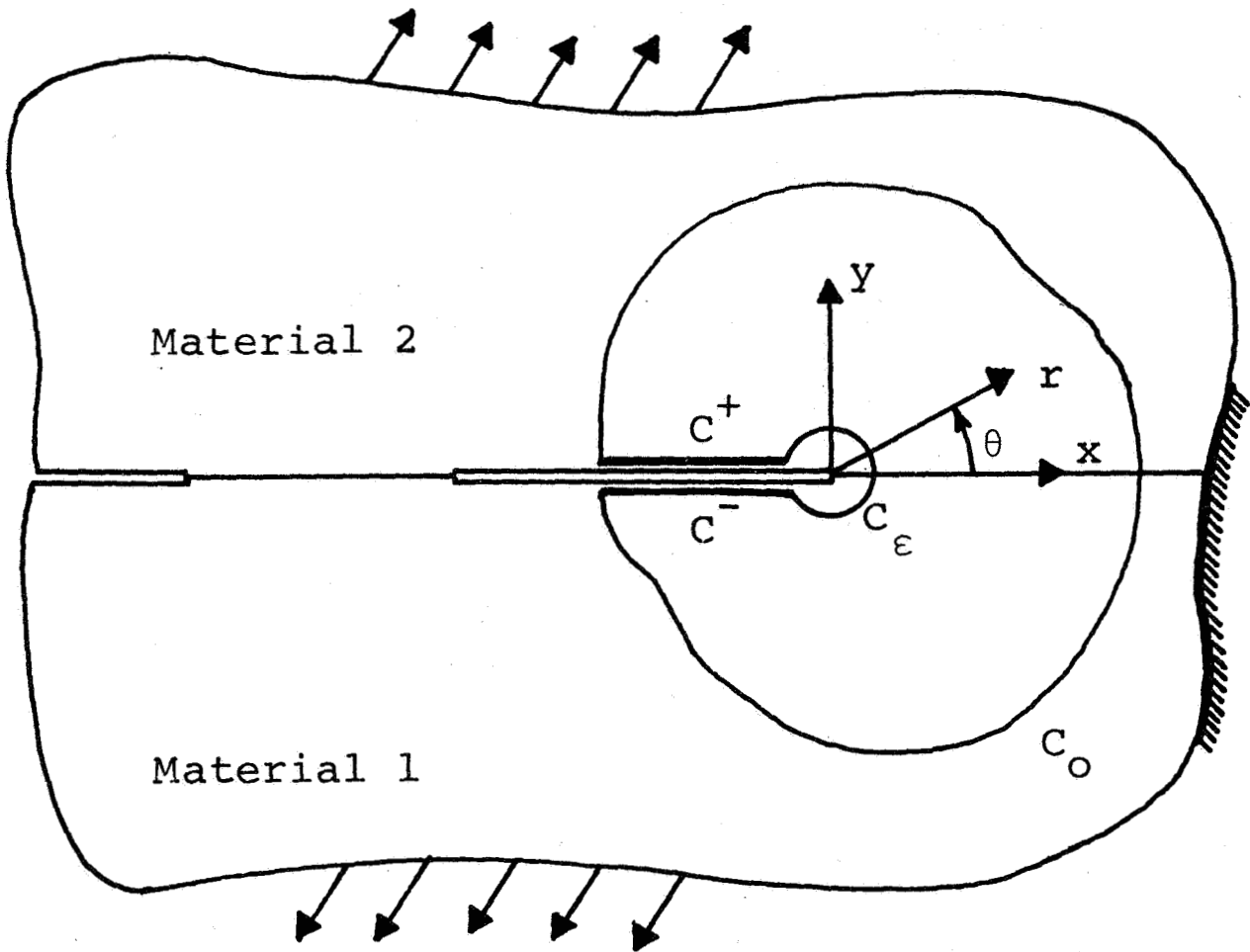
Figure 1.- Basic boundary value problem.

i) Central crack - free edges. ii) Central crack - restrained edges.

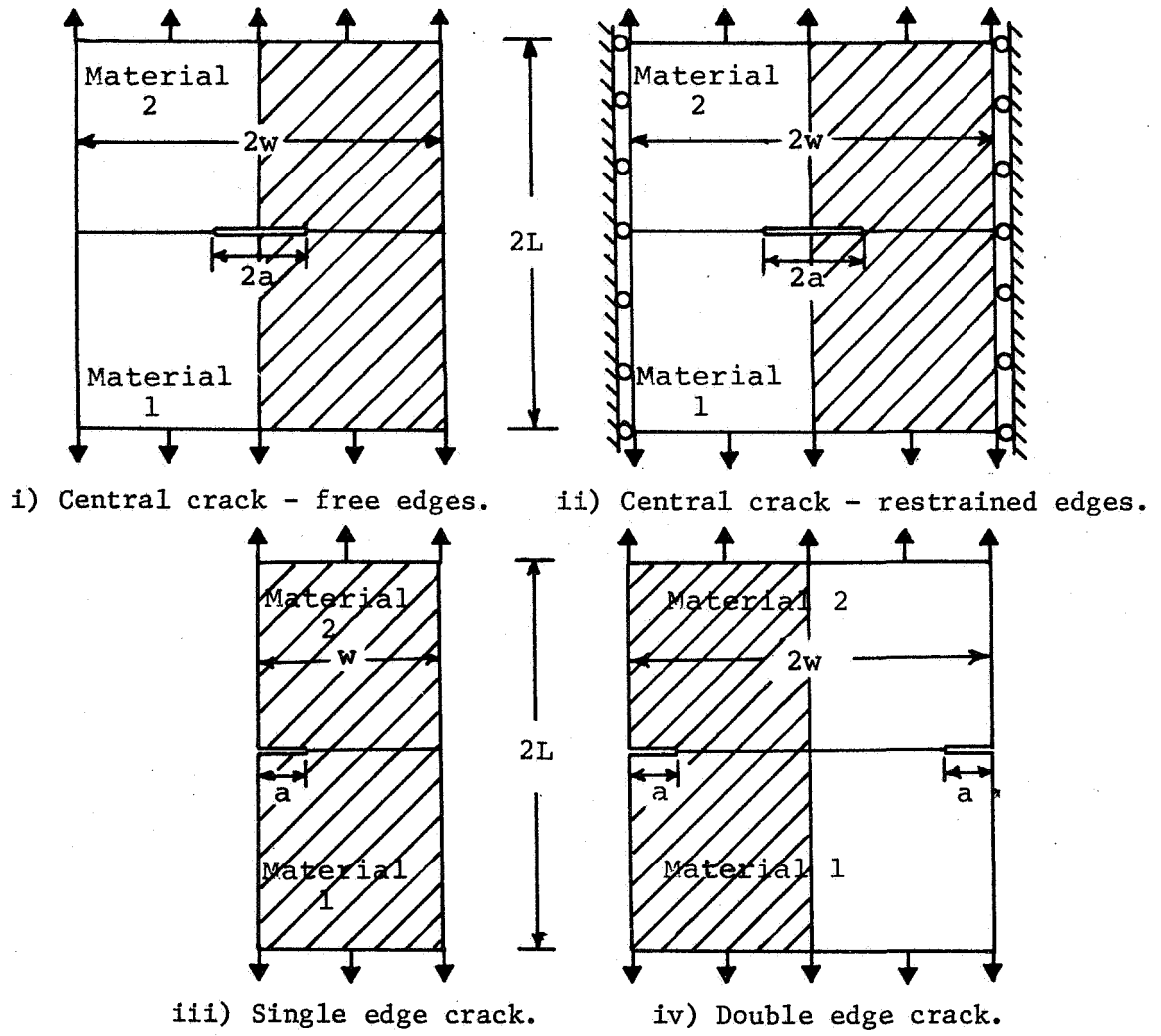iii) Single edge crack. iv) Double edge crack.

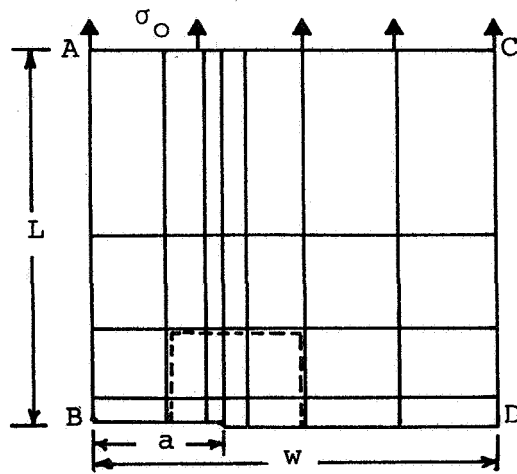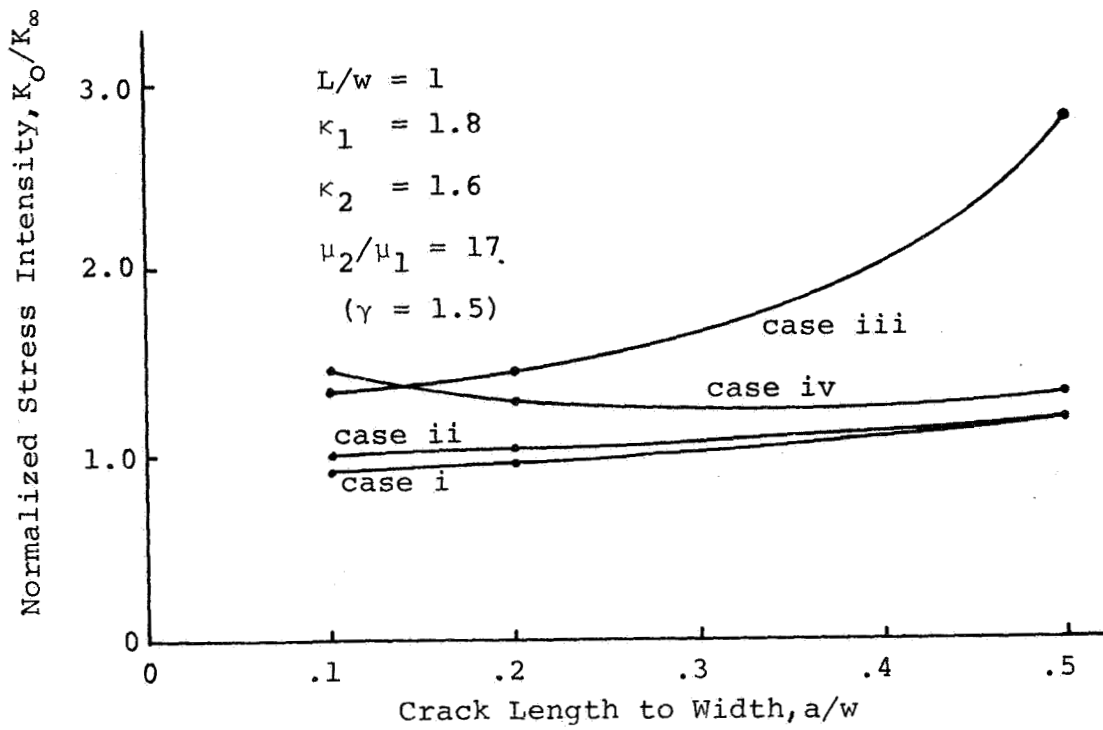Figure 2.- The four cases considered.
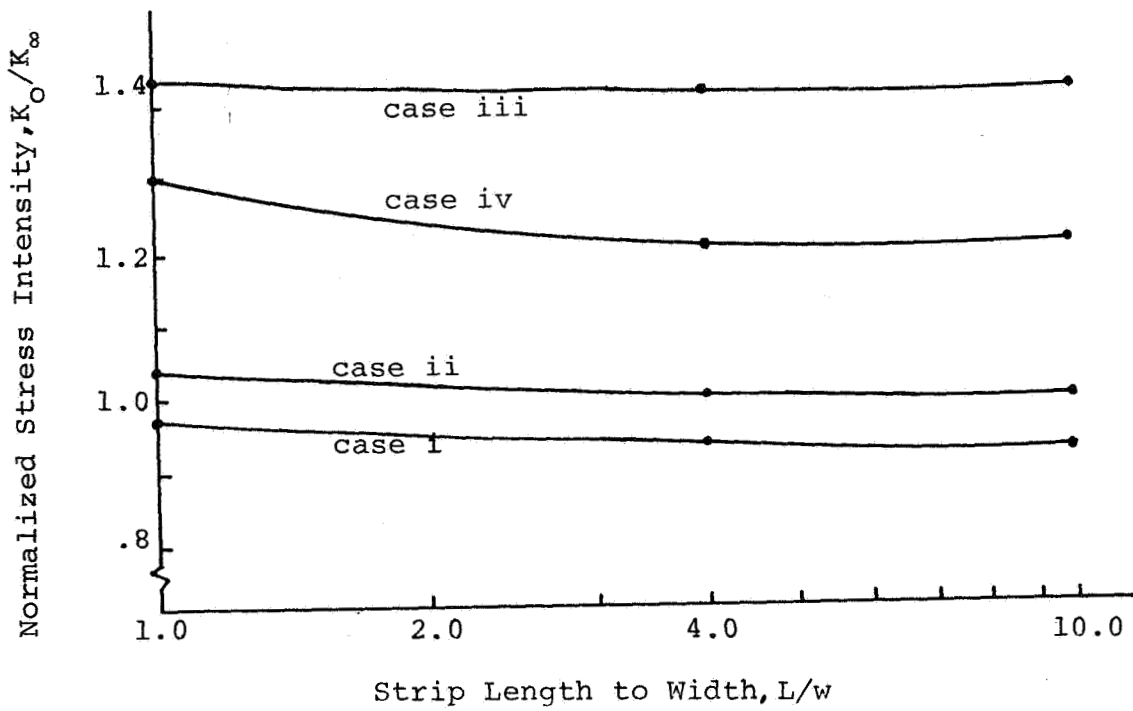

Figure 3.- Finite element grid.

Figure 4.- Effect of crack length.

Figure 5.- Effect of strip length.